Delft University of Technology

Performance Comparison of Single- and Multi-Lobe Antenna Arrays in 5G Urban Outdoor Environments at mm-Waves via Intelligent Ray Tracing

Aslan, Yanki; Puskely, Jan; Roederer, Antoine; Yarovoy, Alexander

Performance Comparison of Single- and Multi-Lobe Antenna Arrays in 5G Urban Outdoor Environments at mm-Waves via Intelligent Ray Tracing

Yanki Aslan[1], Jan Puskely[2], Antoine Roederer[3], Alexander Yarovoy[4]

MS3 Group, Department of Microelectronics, Faculty of EEMCS, Delft University of Technology

Mekelweg 4, 2628 CD Delft, The Netherlands

{[1]Y.Aslan, [2]J.Puskely-1, [3]A.G.Roederer, [4]A.Yarovoy}@tudelft.nl

Abstract—**The effect of forming single and multi-lobe beam patterns at mm-wave base station antennas on the received signal strength and co-channel interference is studied for mm-wave urban outdoor environments. A sample, simplified urban city model is used with randomly selected user positions. Ray tracing simulations are performed to analyze the channel's directional characteristics towards the test users. Depending on the number of dominant paths, single or multiple main lobes are created in the appropriate directions. Through the simulations, it is observed that in comparison with the multi-lobe beam option, the single-lobe beam provides similar or better received power results (unless the ray phases are equalized at the transmitter or receiver with perfect channel information or there is an unexpected sudden blockage in the main path), while providing better interference cancellation capabilities towards other co-channel users.**

Index Terms—**beamforming, fifth generation (5G), mm-wave propagation, pattern shaping, phased arrays, ray tracing.**

I. INTRODUCTION

Approaches to base station (BS) antenna synthesis and beamforming (BF) in future communication systems are expected to be capacity-driven, rather than directivity-driven which has been traditionally used with free-space based performance evaluation metrics [1]. Therefore, it is crucial to incorporate the channel and propagation aspects in the process of selecting the optimal BF strategy in 5G.

Ray tracing is one of the most commonly used methods to identify the directional characteristics of a channel and predict the received signal level for coverage and interference assessments [2]. However, the accuracy of ray phases and amplitudes in ray tracing is limited due to simplifications in the building database. Still, the major interest is in the spatially averaged received power over a small area, which is acceptably approximated in ray tracing by the sum of the ray powers [3].

In [4], using ray tracing, three major BF strategies were studied for mm-wave indoor applications: radial, single and multi BF. In radial BF, the environment is ignored and a beam is created considering the known positions of the BS and the user. As expected, such a strategy has the worst performance among the three. In single BF, the most dominant ray direction of a user is found via ray tracing with an omnidirectional BS antenna and the single-lobe beam with the optimal directivity is steered accordingly. On the other hand, in multi BF, multiple main lobes are formed (towards the first few strongest ray directions) and equalized to focus the power at the user. From the simulations, it was inferred that single BF is the most efficient solution since there is a single dominant path in most of the cases. It was also claimed that multi BF performs as well as single BF in the case of multiple dominant paths and provides additional robustness against sudden changes in the channel (blockage, movement etc.). However, the higher co-channel interference caused by the multiple lobes and the corresponding decrease in the link quality was not discussed.

To the authors' knowledge, there is no prior study that compares the performance of single- and multi-lobe BF in an urban outdoor environment. In this work, we compare the two candidate BF methods in a sample city environment with a focus on their performance regarding the intended received power and the unwanted co-channel interference. The paper is organized as follows. Section II describes the simulation settings. The simulation results and discussions are given in Section III. Section IV presents the conclusions.

II. SIMULATION SETTINGS

The propagation environment, simulation scenario, applied settings and assumptions are summarized as follows:

- Altair HyperWorks WinProp - Propagation Modeling tool [5] is used with the Student License for the three-dimensional rigorous intelligent ray tracing simulations.
- The hybrid ray tracing solver of WinProp is run in the noncoherent (power related, no consideration of phase) mode to plot the received power distributions.
- CST MWS is used to compute the antenna patterns.
- An iterative sampling based pattern matching technique [6] is used in MATLAB in order to find out the excitation coefficients of the shaped (multi-lobed) beam patterns.
- The contribution of rays are given by Fresnel coefficients (for reflection losses) and GTD/UTD (for diffraction losses), based on permittivity, permeability, conductivity and thickness of the materials.
- Reflection from the ground is not taken into account, only the buildings at the fixed positions with the fixed shapes are considered, which is the sample city model "*city.oib*" provided by WinProp (see Fig. 1).
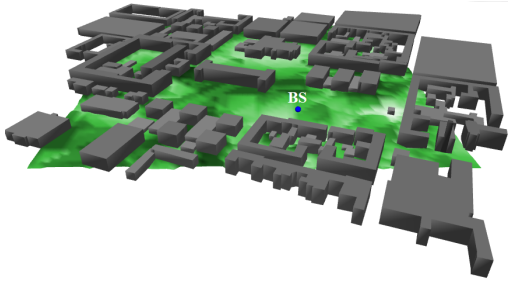- Isotropic antenna at the users is assumed.

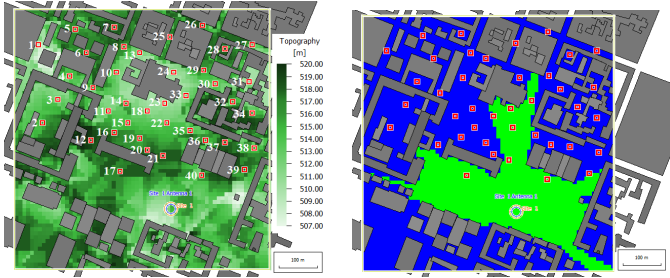Fig. 1. 3D city view with the buildings and the base station (BS).

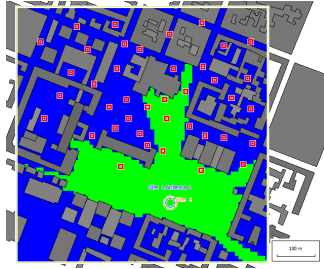Fig. 2. Topography and the positions of test users.

Fig. 3. LoS area.

- The frequency is set to 28 GHz.
- The resolution of the prediction results is 10 meters. In other words, the computation grid is set to 10 meter by 10 meter pixels (cannot be modified).
- Users are located at 2 meter height above the ground with the given topography (the topography or the value of 2 meters cannot be changed). 40 test users are randomly distributed over the city (see Fig. 2).
- Base station is at 15 meters above the ground. There is no tilting in elevation.
- Assumed polarization is vertical.
- Propagation results are filtered using a filter of order 3.
- The buildings are made of concrete with permittivity of 5.31 and conductivity of 0.48 S/m at 28 GHz [7].
- In all simulations, the transmit power is set to 1.6 Watts, assuming 20 dBm power amplifier output per element in a 16 element array. The value of 20 dBm is set considering the state-of-the-art low-cost, silicon-based analog beamforming IC of NXP Semiconductors [8]. Note that in this study, we are interested in the relative changes in the received power at the users for different beamforming strategies at the BS. The true value of the transmit power does not play an important role here.
- Path loss exponent is taken as 2 / 2.4 for LoS / NLoS before the breakpoint and 3.6 / 3.6 for LoS / NLoS after the breakpoint. The breakpoint is set to 500 meters. Note that these values are rough estimates for our test case and the real values should be computed by fitting the ray tracing results to the experiments as performed in [9].
- Possible interaction types are reflections and diffractions.
- Maximum path loss of contributing rays is 200 dB and the maximum dynamic range per pixel is 100 dB.

III. SIMULATION RESULTS

The LoS and NLoS areas are shown in Fig. 3. First, an omnidirectional antenna (with 0 dBi gain) is used at the BS and the received powers of the first 5 strongest rays towards each user are computed. The results are given in Table I. Following the assumption in [4], it is assumed that if the difference between 1st and 2nd ray is larger than 5 dB, there is a single dominant path. Thus, it can be seen that most of the users (30 out of 40) have a single dominant path.

A pin-fed patch element is designed in CST MWS to be used in the array simulations. The design parameters and simulation results of the single antenna element are given in Fig. 4. In this section, the NLoS simulations are grouped into two categories depending on the number of dominant paths and the results are given for several sample user positions.

A. NLoS simulations in the case of having a single dominant path – Users #4, #13, #37

For Users #4, #13 and #37, there is a single dominant path shown in Fig. 5(a). In this case, a single-lobe beam is formed towards this path using progressive phase shifts in a

TABLE I
THE RECEIVED POWERS FROM THE FIRST 5 STRONGEST RAYS TOWARDS EACH OF THE 40 TEST USERS IN THE CASE OF AN OMNIDIRECTIONAL BS ANTENNA.

User #	1st ray (dBm)	2nd ray (dBm)	3rd ray (dBm)	4th ray (dBm)	5th ray (dBm)
1	-131.75	N/A	N/A	N/A	N/A
2	-114.01	-156.26	N/A	N/A	N/A
3	-122.41	N/A	N/A	N/A	N/A
4	-122.28	-160.87	N/A	N/A	N/A
5	-127.80	N/A	N/A	N/A	N/A
6	-123.26	N/A	N/A	N/A	N/A
7	-138.84	N/A	N/A	N/A	N/A
8	-114.48	-114.70	-116.95	-120.25	-151.30
9	-127.03	-130.33	-142.92	-143.32	-144.34
10	-107.74	-112.16	-112.64	-115.34	-115.42
11	-107.84	-108.73	-113.98	-114.49	-114.87
12	-101.99	-104.97	-112.02	-117.87	-120.13
13	-109.24	-138.68	-142.39	-155.02	-159.91
14	-106.47	-108.48	-110.62	-114.80	-118.58
15	-98.15	-103.58	-104.22	-106.94	-107.73
16	-103.16	-108.42	-108.64	-108.93	-113.26
17	-74.26	-88.86	-99.47	-99.66	-100.82
18	-77.51	-97.36	-102.01	-102.24	-104.53
19	-103.89	-106.16	-106.44	-107.29	-109.03
20	-102.77	-103.43	-104.73	-116.39	-117.79
21	-72.88	-94.12	-98.00	-99.93	-103.09
22	-76.58	-100.70	-101.07	-105.42	-118.50
23	-77.97	-96.06	-101.83	-104.55	-106.83
24	-117.30	-140.09	-143.52	-148.80	-149.87
25	-121.56	-137.31	-141.12	-144.70	-156.83
26	-134.30	N/A	N/A	N/A	N/A
27	-137.41	N/A	N/A	N/A	N/A
28	-126.68	N/A	N/A	N/A	N/A
29	-115.97	-117.37	-120.18	-120.36	-124.43
30	-127.84	-155.90	-157.36	-159.10	-161.95
31	-131.07	N/A	N/A	N/A	N/A
32	-119.25	N/A	N/A	N/A	N/A
33	-78.66	-99.12	-113.89	-120.35	-130.61
34	-125.68	N/A	N/A	N/A	N/A
35	-90.49	-96.84	-99.38	-101.01	-103.59
36	-99.72	-102.33	-107.44	-107.77	-112.96
37	-96.18	-101.24	-110.48	-119.59	-123.05
38	-95.19	-103.29	-108.90	-135.05	-135.45
39	-93.96	-101.97	-103.22	-104.74	-110.30
40	-71.03	-88.79	-92.35	-96.69	-99.84

N/A means that the ray path loss is higher than 200 dB.

Green : Single dominant path - LoS.

Yellow : Single dominant path - NLoS.

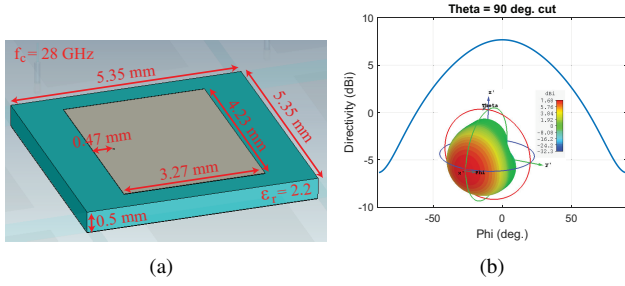Red : Two or more comparable main paths - NLoS.

Fig. 4. Single element in CST: (a) design parameters, (b) directivity.

16-element $\lambda/2$ spaced array of the designed patch antenna. The results are provided in Table II. When compared to Table I, it can be seen that the magnitude of the 1st ray is increased by the amount of the array gain, as expected.

B. NLoS simulations in the case of having two or more dominant paths – Users #8, #11, #14, #20, #29

Here, we will study the effect of using single- and multi-lobe beams (in the 16-element $\lambda/2$ spaced array) on the received power of the users having more than one dominant path.

For User #8, there are two main paths positioned at -3 and -15 degrees off-broadside (see Fig. 5(b)). The single-lobe beams are formed using progressive phase shifts, while beam shaping is applied to form the two-lobe pattern. Fig. 7 provides the excitation coefficients and radiation pattern of the two-lobe beam. The simulation results for User #8 are summarized in Table III. We see that forming a single beam at -3 degrees performs the best in the non-coherent mode, which is followed by the two-lobe beam. This is due to the gain drop in the two-lobe case and the non-significant contribution from the 2nd ray in the single-lobe case, which is also in the direction of -3 degrees with diffraction instead of reflection. In the fully-coherent mode, the two-lobe beam increases the received power only by 0.5 dB as compared to the closest single beam option.

For User #11, the BS antenna is mechanically rotated in azimuth by 25 degrees to steer the broadside and the two main paths are oriented towards ±58 degrees (see Fig. 5(c)). Fig. 8 provides the excitation coefficients and radiation pattern of the two-lobe beam. The simulation results for User #11 are summarized in Table IV. In this case, the two-lobe beam pattern performs slightly better than the single-lobe pattern in the non-coherent mode. The gain drop in the two-lobe beam is compensated by the addition of the ray intensities originated from the two main lobes. In the fully-coherent mode, the two-lobe beam increases the received power by 1.4 dB as compared to the closest single beam option.

For User #14, two strongest paths have a wide angular separation (see Fig 5(d)). In such cases, two (probably out of three or four) sectors can cooperate to serve the user. Fig. 8 provides the excitation coefficients and radiation pattern of the two-lobe beam.

For User #20, the BS antenna is mechanically rotated in azimuth by 45 degrees to steer the broadside and the main paths are oriented towards 38, -43 and -56 degrees (see Fig.

5(e)). A two-lobe (38 and -43 degrees) and a three-lobe (38, -43 and -56 degrees) beams are formed. Fig. 9 and Fig. 10 provide the excitation coefficients and radiation pattern of the two-lobe and three-lobe beams, respectively. The simulation results for User #20 are summarized in Table V. In this case, steering the beam towards the strongest ray direction (38 degrees) provides the best result in the non-coherent mode. However, the total received power values are very close to each other, especially in the case of having a single-lobe at 38 degrees and two-lobes at 38 and -43 degrees. In the fully-coherent mode, the three-lobe beam increases the received power by 3 dB as compared to the closest single beam option. Yet, the interference towards the other users is different in each case. Therefore, the selection of beam position should be made depending on the other users sharing the same time/frequency slot. The received power distribution for each beam position in Table V are given in Fig 6. It is seen that the multiple lobes increase the inter-user interference and in practice, forbids the re-use of the same frequency around the main lobes.

For User #29, two strongest paths are not resolvable for the 16 element array (see Fig. 5(f)). In such a case, a single-lobe beam can cover both paths.

For completeness, the simulations with the two-lobe beams were repeated using the coherent mode of WinProp which takes into account the uncompensated ray phases [10]. It was seen that compared to the non-coherent mode, the received power is 3.9 dB less, 5.4 dB less and 1.5 dB more in the coherent mode for User #8, User #11 and User #20, respectively. This study shows that the result depends very much on the relative phases of the dominant paths. Ideally, with the accurate channel state information at the receiver or transmitter, all the incoming rays should be equalized in time and phase by employing a Rake (at receiver) or Time Reversal (at transmitter) architecture, which yields the fully-coherent field sums in Tables III-V. However, such a case increases the complexity of the system and, as already stated in Section I, does not comply with the limited-accuracy ray tracing simulations.

IV. CONCLUSION

The intended received power and unwanted co-channel interference performances of single-lobe and (adaptively-combined) multi-lobe beam arrays have been studied in a 5G urban outdoor environment at mm-waves. A sample urban city model has been considered with randomly selected user locations. Ray tracing simulations have been performed (at 28 GHz) to compute the ray directions, interactions and intensities. An omnidirectional pattern has been used at the BS to identify the characteristics of the dominant paths towards each user. It has been observed that, in most of the cases, there is only a single dominant path for which the single-lobe beam with the optimal directivity can be steered using a phased array by applying progressive phase shifts. For the users having more than one dominant path, one or multiple main lobes have been formed in the direction of the strongest paths. It has been concluded that, unless the receiver (or transmitter) has
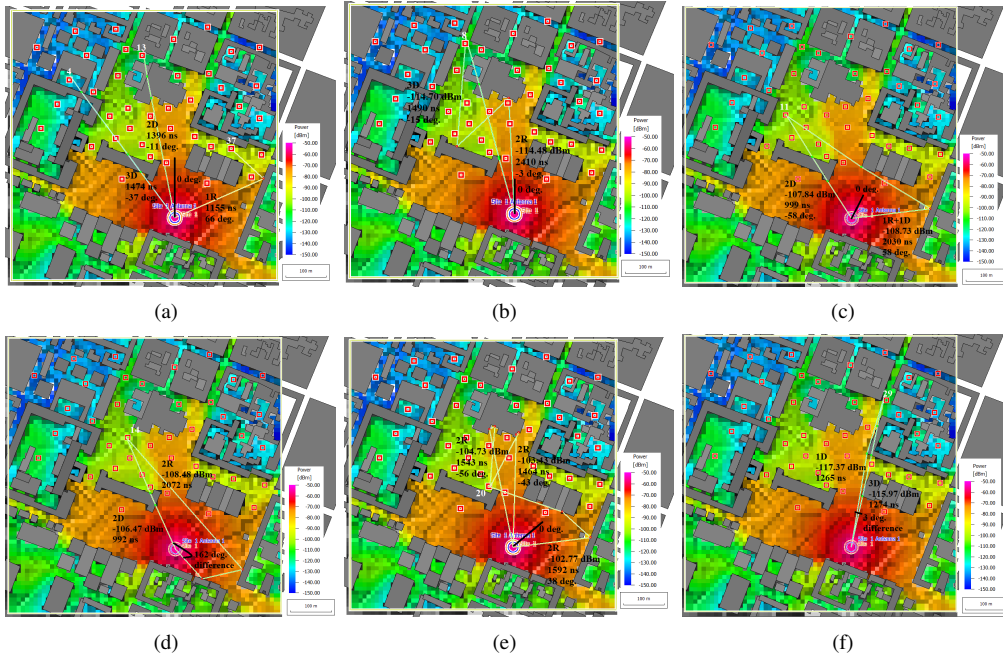
Fig. 5. Interaction type and number, time delay and angle of departures in the case of an omnidirectional BS antenna for Users (a) #4, #13, #37, (b) #8, (c) #11, (d) #14, (e) #20, (f) #29.
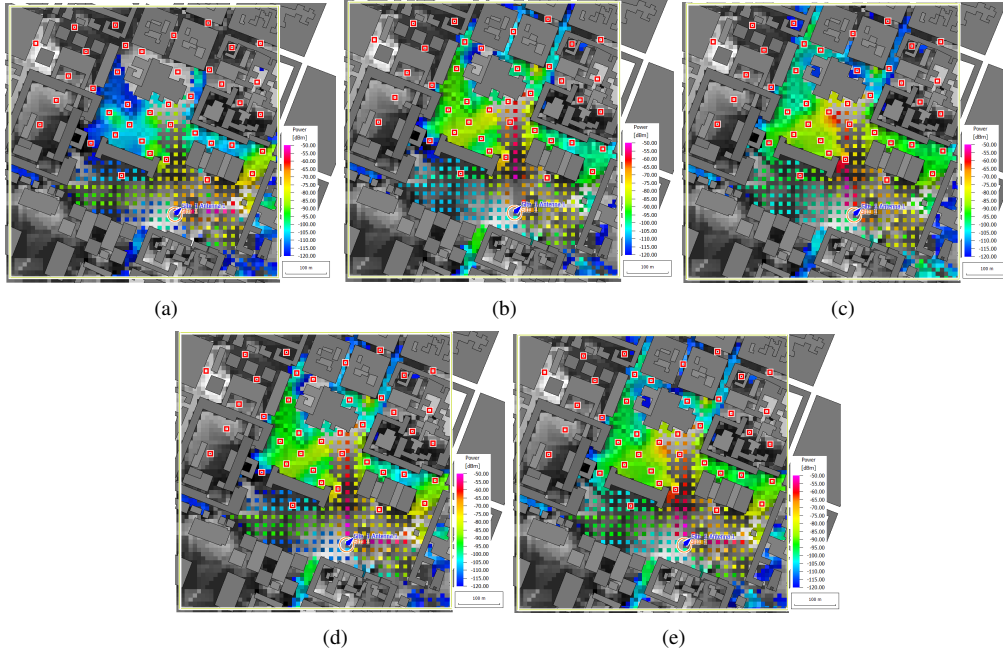

Fig. 6. The distribution of received power at the other (potentially co-channel) NLoS users while serving User #20 with: (a) a single lobe at 38 degrees, (b) a single lobe at -43 degrees, (c) a single lobe at -56 degrees, (d) two lobes at 38 and -43 degrees, (e) three lobes at 38, -43 and -56 degrees *Note: In the case of importing a directional beam, there is a bug in the software which does not allow to see a smooth power distribution in the LoS region.*

the accurate channel state information and a complex Rake (or Time Reversal) architecture to equalize the ray phases, steering a single-lobe beam towards the dominant path could yield comparable or better received powers than the multi-lobe ones which suffer from directivity loss. Besides, the single-lobe beam option generally has a key spectrum efficiency and flexibility advantage over the multi-lobe because it has

optimum interference-cancellation capability towards the other co-channel users. On the other hand, the multi-lobe practice automatically forbids re-use of the same band in and around the other lobe directions. The major advantage of multi-lobe pattern is its spatial diversity that can be helpful in sudden, unexpected blockage of the main path in the direction of the single-lobe beam.

TABLE III

ANGLE OF MAIN LOBES, ARRAY DIRECTIVITIES AND RECEIVED POWERS
FROM THE FIRST 5 STRONGEST RAYS FOR USER #8.

Angle of main lobe(s) (degrees)	Array directivity (dBi)	1st ray (dBm)	2nd ray (dBm)	3rd ray (dBm)	4th ray (dBm)	5th ray (dBm)	Power sum (dBm)	Coherent sum (dBm)
-3	17.80	-96.95	-99.42	-112.47	-134.86	-136.38	-94.92	-91.18
-15	17.71	-97.13	-115.41	-117.89	-120.78	-141.23	-97.01	-94.95
-3 & -15	15.74 & 15.06	-99.42	-99.78	-101.89	-131.27	-138.15	-95.46	-90.64

TABLE IV

ANGLE OF MAIN LOBES, ARRAY DIRECTIVITIES AND RECEIVED POWERS
FROM THE FIRST 5 STRONGEST RAYS FOR USER #11.

Angle of main lobe(s) (degrees)	Array directivity (dBi)	1st ray (dBm)	2nd ray (dBm)	3rd ray (dBm)	4th ray (dBm)	5th ray (dBm)	Power sum (dBm)	Coherent sum (dBm)
-58	16.87	-91.63	-109.78	-112.12	-116.02	-118.79	-91.50	-89.20
58	16.87	-92.30	-98.53	-109.33	-116.08	-119.23	-91.28	-87.50
-58 & 58	14.09 & 14.13	-94.25	-94.77	-101.00	-115.54	-116.12	-91.00	-86.06

TABLE V

ANGLE OF MAIN LOBES, ARRAY DIRECTIVITIES AND RECEIVED POWERS
FROM THE FIRST 5 STRONGEST RAYS FOR USER #20.

| Angle of main lobe(s) (degrees)	Array directivity (dBi)	1st ray (dBm)	2nd ray (dBm)	3rd ray (dBm)	4th ray (dBm)	5th ray (dBm)	Power sum (dBm)	Coherent sum (dBm)
38	17.37	-85.52	-109.64	-110.69	-112.66	-112.91	-85.47	-83.91
-43	17.28	-86.30	-101.65	-107.22	-110.34	-117.71	-86.12	-83.69
-56	16.94	-88.29	-101.08	-104.65	-110.74	-111.44	-87.93	-84.62
38 & -43	14.93 & 14.14	-88.01	-89.36	-104.89	-109.62	-112.13	-85.54	-81.38
38, -43 & -56	12.93, 13.27 & 13.14	-90.09	-91.00	-91.90	-105.01	-114.22	-86.10	-80.68
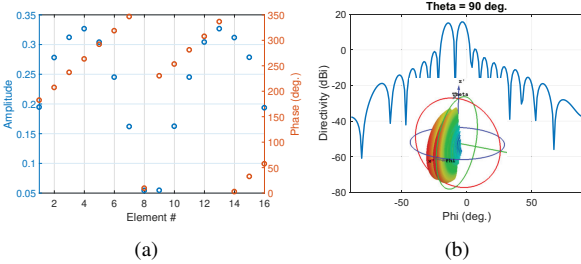
Fig. 7. Two main-lobe 16-element array synthesis for User #8 with beams at
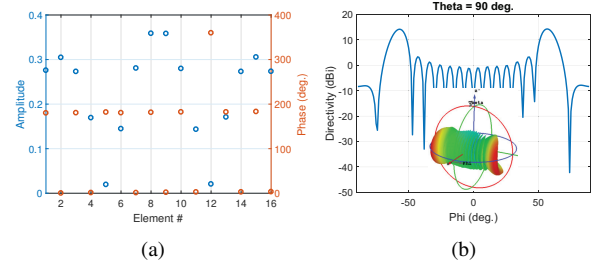-3 and -15 degrees: (a) amplitudes and phases, (b) radiation pattern.

Fig. 8. Two main-lobe 16-element array synthesis for User #11 with beams
at -58 and 58 degrees: (a) amplitudes and phases, (b) radiation pattern.
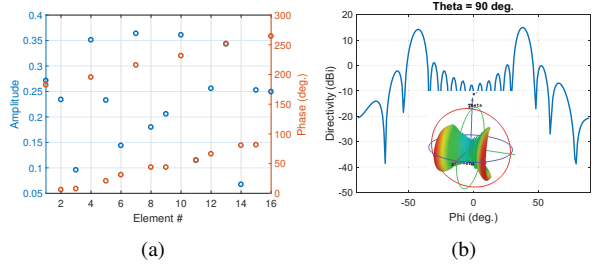

Fig. 9. Two main-lobe 16-element array synthesis for User #20 with beams
at 38 and -43 degrees: (a) amplitudes and phases, (b) radiation pattern.
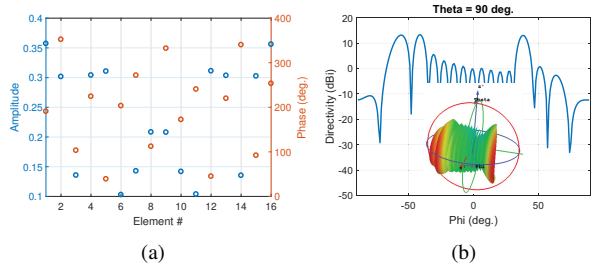

Fig. 10. Three main-lobe 16-element array synthesis for User #20 with beams
at 38, -43 and -56 degrees: (a) amplitudes and phases, (b) radiation pattern.

REFERENCES

[1] G. Oliveri, G. Gottardi, and A. Massa, "A new meta-paradigm for the
synthesis of antenna arrays for future wireless communications," *IEEE
Trans. Antennas Propag.*, vol. 67, no. 6, pp. 3774-3788, Jun. 2019.

[2] A. F. Molisch *et al.*, "Millimeter-wave channels in urban environments,"
in *Proc. 10th EuCAP*, Davos, Switzerland, Apr. 2016.

[3] L. C. Godara, *Handbook of Antennas in Wireless Communications*, CRC
Press, 2002.

[4] V. Degli-Esposti *et al.*, "Ray-Tracing-Based mm-Wave Beamforming
Assessment," *IEEE Access*, vol.2, pp. 1314-1325, 2014.

[5] R. Hoppe, G. Wölfle, and U. Jakobus, "Wave propagation and radio
network planning software WinProp added to the electromagnetic solver
package FEKO," in *Proc. IEEE ACES*, Florence, Italy, May 2017.

[6] W. L. Stutzman, "Synthesis of shaped-beam radiation patterns using
iterative sampling method," *IEEE Trans. Antennas Propag.*, vol. 19, no.
1, pp. 36-41, Jan. 1971.

[7] International Telecommunication Union, "Effects of building materials
and structures on radiowave propagation above about 100 MHz ,"
Recommendation ITU-R P.2040-1 , Jul. 2015.

[8] Y. Aslan *et al.*, "Passive cooling of mm-wave active integrated 5G base
station antennas using CPU heatsinks," in *Proc. 49th EuMC*, Paris, France,
Oct. 2019.

[9] A. M. Bokiye, "Ray-based propagation modeling for OFDM-based
mobile networks," *MSc. Thesis*, Delft University of Technology, The
Netherlands, Jun. 2009.

[10] M. H. Vogel, "MIMO System Simulation in WinProp," *White Paper*,
Altair Engineering, Inc.